Identifying dissolved phosphorus source areas and predicting transport from an urban watershed using distributed hydrologic modeling

Zachary M. Easton,[1] Pierre Gérard-Marchant,[2] M. Todd Walter,[1] A. Martin Petrovic,[3] and Tammo S. Steenhuis[1]

Received 2 November 2006; revised 9 May 2007; accepted 20 July 2007; published 17 November 2007.

[1] A reduction in surface water quality in urban watersheds due to nonpoint source phosphorus (P) loading has prompted municipalities to consider management practices to reduce P loss from landscapes. However, locating P source areas can be time consuming and expensive. Use of distributed models allows delineation of P source areas and focused management strategies. Using the spatially distributed soil moisture distribution and routing model, we adapt and validate a dissolved P (DP) loading model for application to an urban watershed, in Ithaca, New York, to identify P source areas. The model calculates DP loss separately for base flow, impervious surfaces, plant-soil complex, and fertilized areas. The load at the outlet is the sum of P loss from the four components distributed throughout the watershed. Both stream and distributed DP loss were well predicted as indicated by comparison with measured data. The model predicted the largest contribution from plant-soil complexes (36%). Impervious surfaces contributed 10% of the total load but as much as 17% in the winter. More important, the impervious surfaces increased DP losses from the adjacent areas due to runoff from the impervious surfaces saturating the soil, thus increasing runoff losses. Fertilizer contributed substantially following application but decreased rapidly thereafter, a result of conversion from soluble to insoluble P. However, fertilization increased soil P levels, and thus DP losses were higher as a whole (19%). Results demonstrate that correctly predicting the coincidence of P and runoff source areas can be a powerful tool to identify and mitigate contamination of surface waters.

Citation: Easton, Z. M., P. Gérard-Marchant, M. T. Walter, A. M. Petrovic, and T. S. Steenhuis (2007), Identifying dissolved phosphorus source areas and predicting transport from an urban watershed using distributed hydrologic modeling, *Water Resour. Res.*, *43*, W11414, doi:10.1029/2006WR005697.

1. Introduction

[2] Many studies have assessed the impact of agricultural activity on nonpoint contaminant sources [*Puckett*, 1995; *Ekholm et al.*, 2000; *Sharpley et al.*, 2001; *Andraski and Bundy*, 2003], but relatively few studies combined extensive field research with comprehensive modeling to characterize the affects of urban development on surface water quality. Nonpoint source phosphorus (P) runoff to surface waters in urban watersheds is gaining greater scrutiny [*Bannerman et al.*, 1993; *Tilley and Brown*, 1998; *Waschbusch et al.*, 1999; *Tufford et al.*, 2003], as these waters have multiple uses such as drinking water and recreation [*Gachter et al.*, 1998]. Urban development can alter the dynamics of nutrient transport to surface water bodies [*Interlandi and Crockett*, 2003], which can be accompanied by an increase in primary productivity [*Smart et al.*, 1981], and a reduction in water quality. *Hamilton et al.* [2004] found more than 70 percent of sampled urban streams exceeded the USEPA phosphorus goal for preventing nuisance plant growth. Thus there is a need to asses the impact of urban development on water resources.

[3] Impervious surfaces have been implicated as a source of many contaminants in urban environments, and are among the main sources for dissolved P (DP) in many northern climates [*Bannerman et al.*, 1993]. *Tierney and Silver* [2002] state that P application rates to roads in cold climates range from 0.19 g km^{-1} a^{-1} to 1.90 kg km^{-1} a^{-1}, much of which would be available for transport via runoff. Phosphorus from both natural sources such as pollen deposition from trees [*Banks and Nighswander*, 1999; *Hu et al.*, 2001], leaching of P from plant tissue [*Tukey*, 1970; *Sharpley*, 1981; *Dorney*, 1985], and airborne particulate deposition [*Ahn and James*, 2001; *Burian et al.*, 2002], as well as anthropogenic sources such as road sand, deicing materials, or misapplied fertilizer can accumulate on impervious surfaces, making their impact on urban water resources critical to assess.

[1]Department of Biological and Environmental Engineering, Cornell University, Ithaca, New York, USA.
[2]Department of Biological and Agricultural Engineering, Driftmier Engineering Center, University of Georgia, Athens, Georgia, USA.
[3]Department of Horticulture, Cornell University, Ithaca, New York, USA.

0043-1397/07/2006WR005697$09.00

[4] Many municipalities are struggling to find ways to reduce the high levels of DP reaching surface waters [*Meals and Budd*, 1998] from urban areas, however, the sources of DP in a developed area are not readily clear [*Waschbusch et al.*, 1999; *Bannerman et al.*, 1993]. In many cases, relatively small areas of the watershed produce high runoff losses and thus large pollutant loads [*Bannerman et al.*, 1993; *Soranno et al.*, 1996; *Endreny and Wood*, 1999; *Sharpley et al.*, 2001]. Indeed, *Easton et al.* [2007] found runoff losses to be distributed heterogeneously throughout the watershed, and higher in the more urbanized area, making it critical to assess P dynamics spatially. Many urban watersheds comprise a mosaic of land uses varying at a fine spatial scale [*Munroe et al.*, 2005], ranging from impervious surfaces to pervious landscapes like parks, lawns, athletic fields, and golf courses [*Interlandi and Crockett*, 2003]. The impact of each land use varies both spatially and temporally, often independently of each other [*Tufford et al.*, 2003]. A distributed model is therefore needed to predict DP loss from diverse landscapes.

[5] Not many spatially validated distributed models exist for predicting the extent and location of P source areas. Models such as the storm water management model (SWMM) [*Zhang and Yamada*, 1996; *Tsihrintzis and Hamid*, 1998], hydrologic simulation program FORTRAN (HSPF) [*Rahman and Salbe*, 1995] and the soil and water assessment tool (SWAT) [*Hernandez et al.*, 2000], may predict integrated responses such as streamflow and stream P load well in both developed and undeveloped watersheds but cannot realistically capture distributed landscape P loss. Currently, SWAT runoff is based on land use and soil type [*Arnold and Fohrer*, 2005], and not on topography; therefore runoff and pollutant transport on the landscape is only correctly predicted for infiltration excess overland flow and not when saturation excess overland flow from variable source areas (VSA) dominates. Additionally, the hydrologic response units (HRU) in SWAT are defined by the coincidence of land use and soil, which neglects topology within an HRU. Thus critical DP source areas such as near stream areas are not explicitly recognized and unique source areas.

[6] HSPF [*Rahman and Salbe*, 1995] is the one of the most widely used urban models but spatially distributed input is lumped before model runs are made, and therefore distributed results are difficult to interpret. For instance, in the South Creek catchment near Sydney, Australia where HSPF was used to study the impact of urbanization, the accuracy of the predicted P loads for different management scenarios is questionable because of lack of spatial validation [*Borah and Bera*, 2004]. MIKE SHE [*Ahmed et al.*, 2005], is a distributed model capable of capturing spatially variable phenomena, but requires extensive calibration, and the DP predictions have never been compared with distributed data to the best of our knowledge. The soil moisture distribution and routing (SMDR) model is a model that requires little or no calibration, and provides spatially distributed predictions of runoff. SMDR has been shown to provide accurate estimates of integrated watershed responses such as streamflow as well as fully distributed responses such as soil moisture distribution in numerous watersheds in the northeast [*Frankenberger et al.*, 1999; *Kuo et al.*, 1999; *Johnson et al.*, 2003; *Mehta et al.*, 2004; *Srinivasan et al.*, 2005; *Gérard-Marchant et al.*, 2005a; *Easton et al.*, 2007].

[7] The goal of this study is to adapt and further develop a distributed DP loading model to provide useful information for targeted water quality management to reduce P loss in urban areas. We use the validated, spatially distributed, hydrological predictions from SMDR [*Easton et al.*, 2007] as the driver for the DP model. The model presented here is an extension of the work presented by *Gérard-Marchant et al.* [2005a] and *Hively et al.* [2005] adapted for an urban watershed. We adapt their algorithms for P loss from manure to predict P dissolution from fertilizers using a second-order kinetic reaction with runoff loss as a driver and incorporate algorithms for predicting P loss from impervious surfaces. The model is validated both spatially (DP loss in runoff from the landscape) and as an integrated response (stream DP load) by application to a 332 ha urban watershed with shallow sloping soils underlain by a restricting layer using commonly available data.

2. Soil Moisture Distribution and Routing Model Overview

[8] Critical inputs to SMDR include the timing, location and magnitude of saturation excess overland flow, infiltration excess runoff (IER) from impervious surfaces, interflow, and base flow [*Easton et al.*, 2007]. We used SMDR to predict these components for the DP model. SMDR was developed as a management tool to locate areas contributing runoff from transient, shallow, perched water tables with applications to shallow, sloping soils, underlain by a restrictive layer [*Frankenberger et al.*, 1999]. Details of the model as applied to a rural watershed can be found in work by *Gérard-Marchant et al.* [2005a] and in the urban watershed used here by *Easton et al.* [2007]. SMDR incorporates weather data and three primary maps; a digital elevation model, soil, and land use with associated descriptive data to predict runoff and subsurface lateral flows on a 10 m grid and base flow at the outlet. Six soil properties are required as input for SMDR, including porosity, bulk density, depth, field capacity, wilting point, saturated hydraulic conductivity, and percentage of rock fragments (Table 1).

[9] For the urban application used here, impervious surfaces were digitized from a 1 m spatial justified digital orthophotograph quarter quadrangle (DOQQ) of the watershed and the imperviousness degree, ID_{10}, of each 10 m $\times$ 10 m cell was then defined by applying a 10 $\times$ 10 moving window to the 1 m DOQQ [*Easton et al.*, 2007]. Each 10 m $\times$ 10 m cell was assigned a degree of imperviousness, ranging from zero to 100, on the basis of the extent of impervious surfaces in the 100 cells making up the region. Infiltration of precipitation or snowmelt and subsequent storage capacity was then reduced by a representative amount. Since this watershed is not serviced by storm sewers, runoff from impervious surfaces is allowed to reinfiltrate in the neighboring downslope cells. Infiltration excess runoff (IER) from the impervious surface is routed to a cardinal and diagonal downslope neighbor using a D∞ algorithm. If a neighboring cell has available storage capacity a fraction of the IER infiltrates the cell until it becomes saturated, and the rest is routed to the next adjacent downslope neighbor where it can infiltrate if storage is available. In this manner all IER from the impervious

Table 1. Land Use, Hillslope Position, and Selected Soil Properties for the Landscape Sampling Locations in Figure 1

Landscape Sampling Location	Land Use	Slope Position	Soil Properties[a]						
			η, $cm^3\ cm^{-3}$	ρ_b, $g\ cm^{-3}$	z, m	θ_{FC}, $cm^3\ cm^{-3}$	θ_{WP}, $cm^3\ cm^{-3}$	K_S, $m\ d^{-1}$	RFC, %
1	grass right of way[b]	toe	0.57	1.4	0.30	0.41	0.21	2.3	1.1
2	wooded scrub	face	0.61	1.1	0.35	0.36	0.20	2.9	14.1
3	grass well maintained	face	0.52	1.3	0.65	0.34	0.19	6.7	1.1
4	grass poorly maintained	toe	0.57	1.1	0.49	0.39	0.21	2.7	1.1
5	wooded successional	toe	0.50	1.5	0.55	0.32	0.17	4.0	14.8
6	grass well maintained	face	0.49	1.4	1.05	0.20	0.10	6.1	15.4
7	wooded successional	face	0.50	1.3	0.85	0.25	0.14	7.9	13.7
8	grass poorly maintained	toe	0.49	1.4	1.05	0.20	0.10	6.1	15.4
9	grass well maintained	face	0.49	1.3	1.00	0.23	0.10	7.9	16.3

[a]Soil properties are porosity (η), bulk density (ρ_b), depth (z), field capacity (θ_{FC}), wilting point (θ_{WP}), saturated hydraulic conductivity (K_s), and rock fragments (RFC).
[b]Landscape sampling location 1 is closest to the watershed outlet.

surfaces is allowed to reinfiltrate given adequate soil storage. We assumed that once runoff is created on pervious surfaces it is routed to the stream within the time step, with no reinfiltration, which we assumed would add little error because of the VSA hydrology [*Easton et al.*, 2007].

3. Dissolved Phosphorus Model Development

[10] Correctly predicting distributed DP loss is complex because of the numerous mechanisms governing transport of P in the environment [*Sharpley et al.*, 2002; *Hively et al.*, 2005], including biotic and abiotic factors [*Frossard et al.*, 2000], such as land use [*Beauchemin et al.*, 1996; *Meals and Budd*, 1998]; soil test P [*McDowell and Sharpley*, 2003; *Mamo et al.*, 2005]; soil particle distribution and mineralogy [*Ekholm et al.*, 2000]; erosion [*Sharpley et al.*, 2002]; landscape fertilization [*McDowell et al.*, 2001; *Andraski and Bundy*, 2003]; P source and rate [*Tarkelson and Mikkelsen*, 2004]; plant uptake [*Norton and Fisher*, 2000]; soil type [*Djodijc et al.*, 2004]; management [*Tilley and Brown*, 1998]; macropore flow [*Hooda et al.*, 1999]; soil P accumulation [*Cassell et al.*, 1989]; sorption kinetics [*Beauchemin et al.*, 1996]; and temperature and precipitation [*Evans and Johnes*, 2004].

[11] Despite the numerous processes mentioned above, there are several that tend to dominate DP loss from urban landscapes. One such process is P loss from fertilizers applied to lawns, which is dominated by the dissolved form [*Garn*, 2002; *Kussow*, 2007]. Indeed, *Easton and Petrovic* [2007] found DP to be 76% of the total P lost from fertilized lawns in Ithaca, NY, while *Nichols et al.* [1994] measured >95% of total P as dissolved from fertilizer applied to tall fescue. Several studies have shown sediment losses to be minimal from well vegetated sites such as home lawns, which are often abundant in urban watersheds [e.g., *Gross et al.*, 1991; *Linde and Watschke*, 1997]. Impervious surfaces, also abundant in urban watersheds, are a clear source of contaminants because of their runoff producing potential [*Dougherty et al.*, 2006] and the associated reduction in biophysical remediation [*Dougherty et al.*, 2007], and are thus considered in our model. Much research has shown high soil P levels create the potential for high dissolved P loss in runoff [*Edwards and Daniel*, 1994; *Sharpley et al.*, 2002; *DeLaune et al.*, 2004a]. Additionally, there is some evidence that P leached from the plant canopy can contribute to P loss in runoff [*Sharpley*, 1981; *Dorney*, 1985], thus the contribution of P mobilized from well vegetated landscapes and lost via runoff from the plant-soil complex represents another potentially large source of P and is thus considered in the model. These processes are described below. The spatially distributed runoff, interflow, and base flow volumes predicted by SMDR are used as driver fluxes in the transport model [*Easton et al.*, 2007], which was created outside of the SMDR framework.

3.1. Dissolved P Loss From Fertilized Areas

[12] There are two pathways for the loss of DP from fertilizer namely, loss in runoff and conversion of soluble P into less soluble forms by interaction with the soil and vegetation. The work of *Sharpley et al.* [1978] and an examination of data from *Easton and Petrovic* [2004, 2007] showed that following application, available fertilizer P declined following an exponential curve, namely,

$$M_{F,t} = M_{F,t-\Delta t} \exp\left(-\frac{\Delta t}{\tau}\right) - D_{F,t-\Delta t} \quad (1)$$

where τ is the immobilization rate (d), $M_{F,t}$ is the available water extractable P at time t per unit area (kg m^{-2} d^{-1}), $M_{F,t-\Delta t}$ is the water extractable P on the previous time step (kg m^{-2} d^{-1}), and $D_{F,t-\Delta t}$ is the fertilizer DP loss in runoff (kg m^{-2} d^{-1}) from the previous time step. Following fertilizer application, the water extractable P in the fertilizer, (a fraction, ω, of the total fertilizer P, M_T, (kg m^{-2}) in the fertilizer) is added to the amount already present on the soil surface. A time step, Δt, of 1 d is used in the model.

[13] The loss of fertilizer DP at time t in runoff ($D_{F,t}$) on each fertilized cell in the watershed is modeled as a second-order kinetic reaction, i.e., $dD_{F,t}/dR_t = k_F M_{F,t}^2$ from *Gérard-Marchant et al.* [2005b], who used the derivative with respect to time for steady state rainfall to model the dissolution of soluble P from manure, i.e., dD_F/dt. Our testing on several data sets [*Easton and Petrovic*, 2004, 2007] indicates that using the derivative of D_F with respect to runoff, R_t (m^3 m^{-2} d^{-1}) would result in the same outcome for a single rainfall with a characteristic volume,

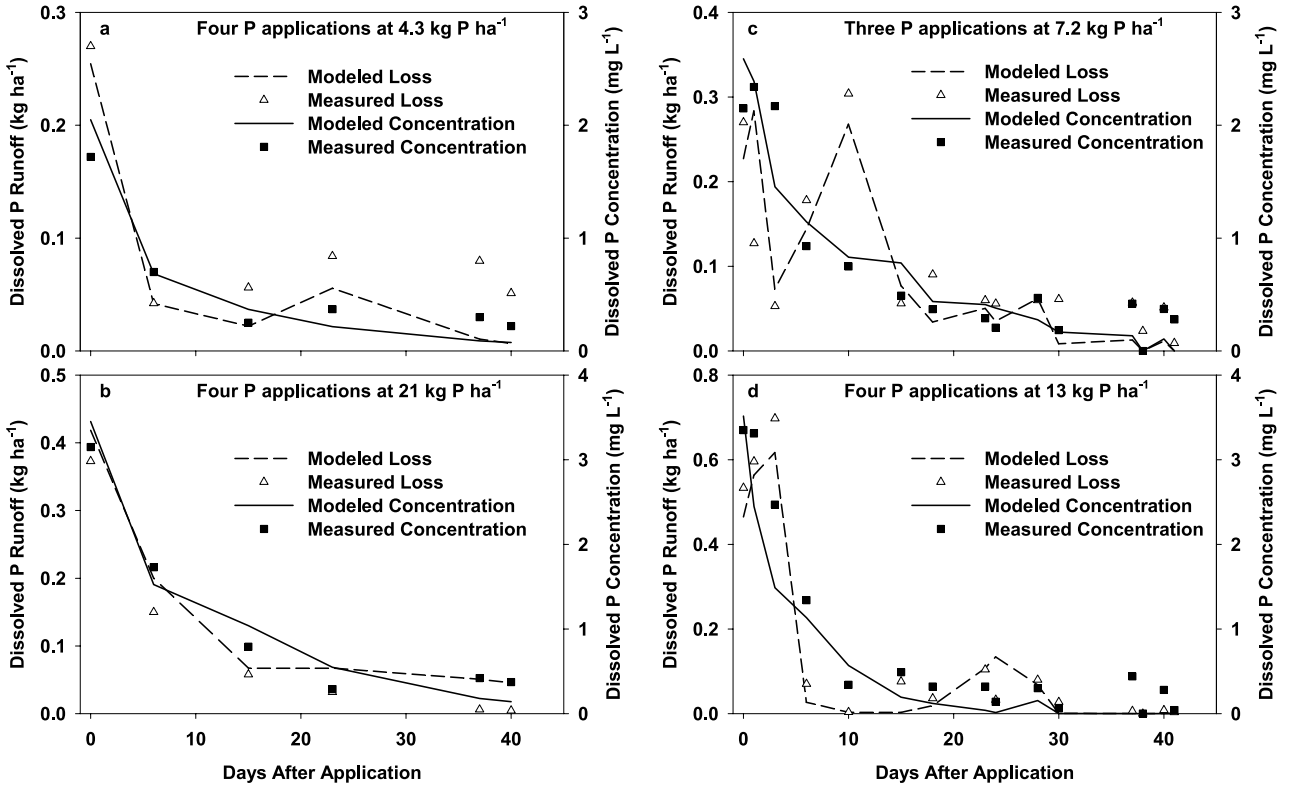

Figure 1. Data from *Easton and Petrovic* [2004, 2007] used to build and test the fertilizer dissolution/loss model. (a and b) Data from *Easton and Petrovic* [2004] were collected on 1 m^2 plots fertilized at four P rates (high and low rate shown) for the second year of the study. (c and d) Data from *Easton and Petrovic* [2007] were collected on 4 m^2 fertilized plots at two P rates in the study watershed during the summer of 2003. We used observed runoff losses in equation (3) for model building and testing; for application in this study, SMDR predicted runoff losses were used.

but gives better results for variable storms. Assuming that the available P ($M_{F,t}$) is equal to M_F before runoff starts, then DP lost during an event is

$$\frac{dD_{F,t}}{dR_t} = k_F\left[M_{F,t} - D_{F,t}\right]^2 \tag{2}$$

where k_F (m^3 kg^{-1}) is the reaction constant. By integrating equation (2) the DP loss from fertilizer, in runoff for each fertilized cell becomes

$$D_{F,t} = \left[M_{F,t}\left(\frac{k_F M_{F,t} R_t}{1 + k_F M_{F,t} R_t}\right)\right] \tag{3}$$

[14] Figure 1 shows data from *Easton and Petrovic* [2004 and 2007] used to derive and test the fertilizer dissolution/loss model. The second year of data from *Easton and Petrovic* [2004] and data from 2003 in work by *Easton and Petrovic* [2007] were used. Runoff was collected from natural rainfall events following fertilization with P application rates ranging from 4.3 to 21 kg ha^{-1}. Orthophosphate was the P source in all fertilizers. The model accurately captured the rapidly declining P concentrations in runoff following application (Figure 1); with a coefficient of determination (r^2) of 0.66. Runoff P losses are also relatively well predicted, but dependent upon both the concentration of P (or available P) and the runoff volume. Thus there is some variation in P runoff losses after applications (Figure 1), still the r^2 = 0.77 indicated adequate model performance.

3.2. P Loss From Plant-Soil Complex

[15] P release from the plant-soil complex reflects both abiotic (sorption/desorption kinetics, soil moisture, temperature, precipitation) and biotic (organic matter mineralization, plant uptake) factors varying with climate and season [*Hansen et al.*, 2002], which makes process-based modeling difficult, and in many cases seemingly impossible. Lumping the relevant processes governing P release from the plant-soil complex for each cell with an export coefficient approach can yield accurate predictions [*Hively et al.*, 2005] with out requiring extensive input data or calibration [*Beven*, 1996], but may not elucidate processes controlling P loss from the plant-soil complex.

[16] We used an export coefficient model, which aggregates the relevant processes affecting P loss by using the mean expected P concentration in runoff from a homogeneous area [*Winter and Duthie*, 2000; *Sharpley et al.*, 2002; *Torrent and Delgadao*, 2001] to predict P loss form the plant-soil complex. A simple linear relationship between the

soil test P (STP) and DP in runoff was used to approximate DP loss from soil via runoff [*Hively et al.*, 2005] as

$$D_{S,t} = \mu_S M_S R_t \tag{4}$$

where $D_{S,t}$ is the daily DP load in runoff (kg m^{-2} d^{-1}), M_S is the soil test P in the surface soil (kg m^{-3}) at time t, R_t is the SMDR predicted runoff (m^3 m^{-2} d^{-1}) from the cell at time t and μ_S is the soil specific coefficient determined from sampled runoff events adjusted for temperature with an Arrhenius equation [*Zheng et al.*, 2003]:

$$\mu_S = \mu_{T,S} Q_S^{\left[\frac{T-T_R}{10}\right]} \tag{5}$$

where $\mu_{T,S}$ is the reference export coefficient, Q_S is a factor change rate for a 10°C change in temperature (varies between 1 and 5 by calibration), T is the average temperature at the soil surface (C°) at time t, and T_R is the reference temperature (C°) at which $\mu_{T,S}$ was estimated. For short durations (i.e., when M_S is assumed to not change) equation (4) simplifies to

$$D_{S,t} = k_S R_t \tag{6}$$

where $k_S = \mu_S M_S$ is the temperature dependent DP export coefficient (kg m^{-3} d^{-1}). Thus k_S is dependent on soil characteristics, temperature, and management factors affecting the P levels in the soil [*Hively et al.*, 2005].

3.3. P Loss From Impervious Surfaces

[17] An accumulation/wash-off equation is used to model the contribution of DP from impervious surfaces [*Sartor and Boyd*, 1972; *Shaheen*, 1975]. The contribution of the various impervious areas to DP stream loads vary both spatially (e.g., roadways contributing higher P loads than roofs), and temporally (e.g., higher contribution in the winter and lower in the summer). Thus the rate of P buildup was allowed to vary on the basis of the presence of snowfall in the watershed. This allows more rapid accumulation of P on the impervious surfaces from the application of deicing materials, consistent with measurements taken in the watershed during winter snowfall events. Accumulation is modeled with an exponential buildup equation:

$$M_{I,t} = M_{I,Max} - \left(M_{I,Max} - M_{I,(t-\Delta t)}\right)[\exp(-k_I \Delta t)] \tag{7}$$

where M_I is the DP load (kg m^{-2}) on the impervious surface, $M_{I,(t-\Delta t)}$ is the P load (kg m^{-2}) from the previous event, $M_{I,Max}$ is the maximum DP load (kg m^{-2}) on the impervious surface, and k_I is the exponential buildup factor (d^{-1}).

[18] Wash-off of DP from the impervious surfaces is estimated using a first-order relationship:

$$D_{I,t} = M_I\left[1 - \exp\left(-k_{I,R} R_t\right)\right] \tag{8}$$

where $D_{I,t}$ is the DP load (kg m^{-2}) in runoff from the impervious surface, $k_{I,R}$ is the wash-off coefficient (m^2 m^{-3}), and R_t is the SMDR predicted IER (m^3 m^{-2}). $D_{I,t}$ is subtracted from $M_{I,t}$ before the next day is calculated. Runoff from impervious surfaces was allowed to reinfiltrate in the surrounding landscape, thus R_t is runoff that could not be assimilated by the surrounding soil and was calculated as the difference between a model run allowing for reinfiltration and a model run with no reinfiltration of IER.

3.4. P Loss in Base Flow

[19] Base flow, although it does not contain high P concentrations, can act as a constant background source of P [*McDowell et al.*, 2001], and contribute substantially to cumulative P loads [*Maguire and Sims*, 2002]. For example *Caruso* [2000] found base flow P exports to be 47% of the P lost from an agricultural watershed, while *Hively et al.* [2005] found base flow P exports to be 30% of the total in a dairy farm dominated watershed. Additionally, soils exhibiting macropore flow can contribute significant P loads to the subsoil, or directly to groundwater [*Hooda et al.*, 1999], thus increasing the base flow P contribution, especially in tile drained watersheds. In an urban area base flow P may be an artifact of in stream processes that mobilize P sequestered in the streambed. Since subsurface geology, climate, land use, and land management [*Wayland et al.*, 2003] can all affect base flow P loss, and much of this information is unavailable for distributed input, a lumped export coefficient approach is used to model base flow P loss:

$$L_{B,t} = \mu_B B_t \tag{9}$$

where $L_{B,t}$ is the DP load (kg d^{-1}) in base flow, B_t is the SMDR predicted base flow volume at the watershed outlet (m^3 d^{-1}), and μ_B is the base flow DP export coefficient adjusted for temperature with an Arrhenius equation similarly to soils (equation (5)):

$$\mu_B = \mu_{T,B} Q_B^{\left[\frac{T-T_B}{10}\right]} \tag{10}$$

where $\mu_{T,B}$, Q_B, and T_B are calibration parameters. Since base flow originates from deeper in the soil profile than surface runoff, the T_B parameter should reflect the greater temperature damping observed at a greater soil depth. Thus the soil temperature measured at 50 cm was used, as it represents one half of the average profile depth [*Hively et al.*, 2005]. Since the base flow coefficient, μ_B, integrates the effects of the entire watershed on DP loss it should be calibrated from observed base flow DP concentrations.

3.5. Stream DP Loss

[20] Now that we have calculated the contributions from fertilizer ($D_{F,t}$), the plant-soil complex ($D_{S,t}$), impervious surfaces ($D_{I,t}$), and base flow ($L_{B,t}$) we sum the loads at the outlet to predict the DP load in the stream ($L_{T,t}$) (kg d^{-1}):

$$L_{T,t} = L_{B,t} + \sum_{n=1}^{i} A\left(D_{F,t} + D_{S,t} + D_{I,t}\right) \tag{11}$$

where A is the area of the of each modeled process.

4. Watershed Description

[21] The model is parameterized and validated in a 332 ha urbanizing watershed located in Ithaca and Lansing, New York (42°48′N, 76°46′W), in the Appalachian Plateau physiographic province (Figure 2). The region is typified

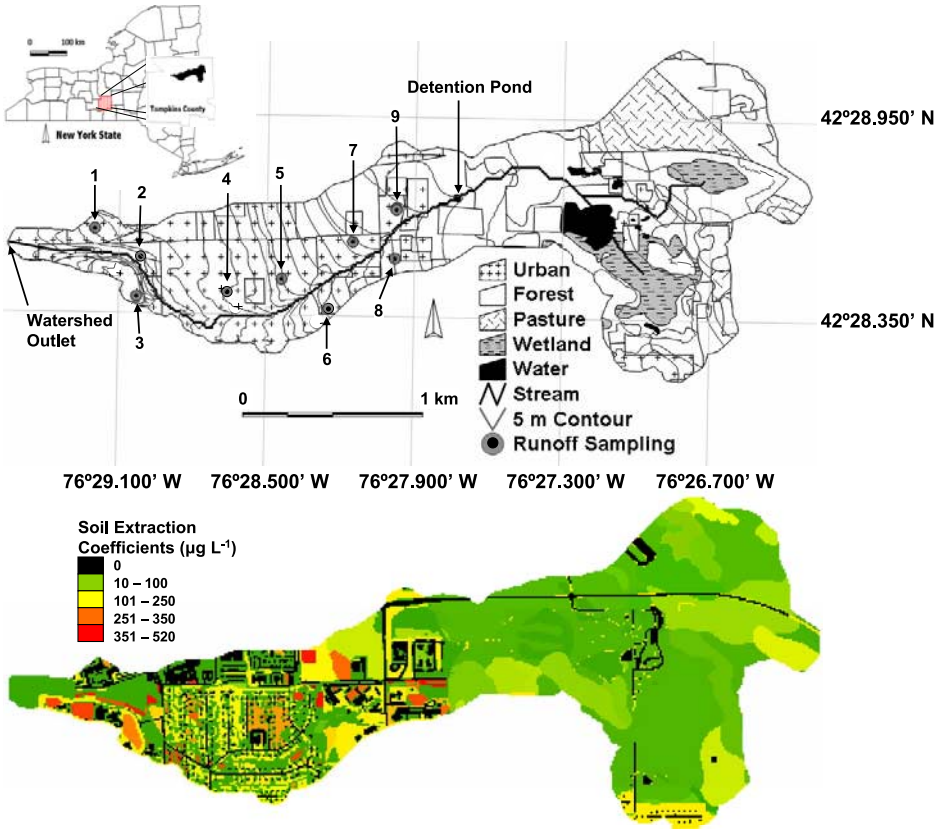

Figure 2. (top) Watershed location in New York State, land use, and 5 m contours with location of landscape sampling plots. (bottom) Soil extraction coefficient map of the watershed. Impervious areas are shown in black on the bottom map, and thus there is no contribution from soil and no extraction coefficient.

by steep hillslopes with flattened hilltops of glacial origins with shallow permeable soils, underlain by a restrictive layer. The climate is humid with an average annual temperature of 7.7°C and average annual precipitation of 1143 mm. Elevation in the watershed ranges from 250 to 350 m above mean sea level with an average slope of 8.5% and slopes as steep as 27% mainly near the watershed outlet. Slopes in the upper watershed are between 2 and 5%. Soils are generally deeper in the upper reaches of the watershed and underlain by bedrock at depth greater than 1 m while soil depth is less near the watershed outlet and underlain by fragipan at depths between 30 and 80 cm (e.g., coarse-loamy, mixed, active, mesic, to frigid Typic Fragiudepts, Lytic or Typic Dystrudepts common to glacial tills). The lower watershed is predominantly urban (40% of total watershed) while the upper watershed is forested (44%), water/wetland (8%), and pasture (8%) (Figure 2). The urban area is a mix of home landscapes (lawns, woods, and impervious areas) as well as parks, schools, and commercial development. Impervious surfaces comprise 24% of the lower watershed (i.e., between the detention pond and outlet in Figure 2).

[22] The overall watershed outflow was measured with an ISCO 6712 stream gauge with a 750 area velocity module (ISCO Inc., Lincoln, Nebraska) (Figure 2). During the growing season rainfall was recorded in the watershed on a 10-min interval with two tipping bucket rain gauges (ISCO Inc., Lincoln, Nebraska). Temperature, winter snowfall, winter rainfall, and nongrowing season calculated evapotranspiration (ET) (Penman-Monteith method) were recorded hourly at a location 3 km south east of the watershed outlet. During the growing season (May–October) pan ET was estimated with a class A pan at a location 5.5 km south east of the watershed outlet. A pan factor of 0.8 was used to determine potential ET. Streamflow samples were collected on 1000–8000 m^3 intervals, providing a nearly complete daily record. During storm event several samples were collected. Samples were filtered through a 0.45-μm filter, and molybdate soluble reactive orthophosphate was determined colorimetrically by ascorbic acid method [*Murphy and Riley*, 1962].

5. Landscape Sampling

[23] For validation of the model nine landscape runoff sampling locations consisting of three landscape types (fertilized areas, unmaintained landscapes, and wooded areas, Table 1) were established on 7–11% slopes in the watershed and a runoff sampler installed (Figure 2). Runoff was collected from a 4 m^2 area (2 m × 2 m) at the locations shown in Figure 2 on the down gradient side of the plot using an H flume and directed to a tipping bucket sensitive to 0.1 mm. Plots were bordered to prevent runoff entering from upslope areas. Ninety eight runoff events (>0.1 mm) were collected from April 2003 to April 2005. Selected runoff events from 2003 were used to calibrate the model. Several runoff events not used for calibration representing a

Table 2. Model Parameter Values Estimated A Priori and A Posteriori

Parameter	Description	Equation	Value	Units
	Estimated A Priori			
M_F	initial water extractable phosphorus in fertilizer	(1), (2)	5.4×10^{-4}	kg m^{-2}
τ	DP immobilization rate	(1)	9.3	d
T_R	base temperature, soil	(6)	20	°C
T_B	base temperature, base flow	(10)	17	°C
$M_{I,Max}$	maximum DP accumulation on impervious surface	(7)	2.5×10^{-4}	kg m^{-2}
k_I	DP exponential buildup factor	(7)	6/2[a]	d^{-1}
$k_{I,R}$	DP wash-off coefficient	(8)	0.02	m^2 m^{-3}
k_F	reaction constant	(2), (3)	0.015	m^3 kg^{-1}
	Estimated A Posteriori			
Q_B	Q_{10} base coefficient, base flow	(10)	2.20	-
$\mu_{T,B}$	reference DP base flow export coefficient	(10)	2.1×10^{-5}	-
Q_S	Q_{10} base coefficient, soil	(6)	1.35	-

[a]The exponential buildup factor was allowed to vary from 6 d^{-1} during the summer to 2 d^{-1} during the winter on the basis of the presence of snowfall in the watershed.

range in seasons and conditions were selected for validation of the distributed modeled landscape DP loss. Landscape runoff samples were analyzed identically to streamflow samples.

6. Parameter Estimation and Calibration

[24] In this model the variables that affect DP concentration in the surface runoff are land use, soil test P, degree of imperviousness, time since fertilizer application, and temperature. The parameters that must be estimated for the DP loading model are: the immobilization rate (τ) (equation (1)), the reaction constant (k_F), water extractable P (M_F), (equation (2)), base temperatures for soil (T_S) (equation (5)), and base flow (T_B) (equation (10)), the maximum DP load that can accumulate on impervious surfaces ($M_{I,Max}$) (equation (7)), the exponential buildup factor (k_I) (equation (7)), the wash-off coefficient ($k_{I,R}$) (equation (8)), the base coefficients for soil (Q_S) (equation (5)) and base flow (Q_B) (equation (10)), and the reference base flow export coefficient ($\mu_{T,B}$) (equation (10)) and soil ($\mu_{T,S}$) (equation (5)). The first year of the study data (2003–2004) were used for calibration, and the following year of data (2004–2005) were used for validation of the model results. The only variable that was calibrated for the hydrologic inputs from SMDR was the temporal distribution of base flow; no others require calibration [*Easton et al.*, 2007]. Most parameters for the DP model were estimated from field measurements, or values reported in the literature. However, some parameters were obtained by model calibration, specifically the coefficients for base flow, Q_B (equation (10)), and soil, T_S (equation (5)), but were not varied spatially. Table 2 summarizes estimated and calibrated parameter values. The sources for the estimates follow.

[25] Fertilized landscapes were identified by a survey of the watershed during summer 2003. The fertilizer P source, application rate, and timing were based on records from two landscaping companies responsible for fertilization of approximately 15% of the fertilized landscapes, and one large watershed land owner (4% of the watershed). On the basis of these records, the average P application rate was 28×10^{-4} kg m^{-2} a^{-1} split into three applications (May, August, and October) making the maximum amount of P per application 9.3×10^{-4} kg m^{-2}. In each application the initial water extractable P (M_F) was set a priori to 55% or 5.4×10^{-4} kg P m^{-2} and the immobilization rate (τ) (equation (1)) was set to 9.3 d on the basis of fertilizer source and solubility. Data on fertilizer solubility and immobilization were abstracted from fertilizer labels. We identified many individual home lawns that were fertilized and assumed that their P application rates were the same as those sources identified above. While this is clearly a simplification, the P application rates used above are within recommended rates for home lawns of New York State.

[26] The plant-soil complex export coefficients, μ_S, were based on STP values from the topsoil, and measured DP concentrations in runoff from 2003–2004 [*Sharpley et al.*, 2002; *Maguire and Sims*, 2002; *McDowell and Sharpley*, 2003; *DeLaune et al.*, 2004b]. Soil test phosphorus was measured twice in 2003–2004 and determined using the Morgan soil test extract [*McIntosh*, 1969], and ranged from 3.7 to 18.5 mg kg^{-1}, low to high on the Morgan scale. Measured STP values from the nine landscape sampling locations (Figure 2) were regressed on DP concentrations from natural runoff events in 2003–2004. The observed STP levels were found to be well correlated ($r^2 = 0.76$) with observed DP concentrations in runoff (mg L^{-1}) ($P_{obs} = 0.11 + 0.06$ STP). The STP/runoff DP regression was used to estimate the DP export coefficients (μ_S) (equation (4)) in overland flow for the remaining soils in the watershed by sampling STP at 68 points in the watershed. Export coefficients were further adjusted on the basis of soil, topology, and land use/management. A 10-m raster map incorporating this information was developed to assign reference DP export coefficients ($\mu_{T,S}$) (equation (5)) (Figure 2).

[27] The maximum DP accumulation on impervious surfaces ($M_{I,Max}$) (equation (7)) was set at 2.5×10^{-4} kg m^{-2} on the basis of measurements taken on impervious surfaces in the watershed and values from the literature [*Tukey*, 1970; *Sharpley*, 1981; *Dorney*, 1985; *Ahn and James*, 2001; *Tierney and Silver*, 2002]. The exponential buildup factor (k_I) (equation (7)) was allowed to vary between 6 d^{-1} for nonsnow periods to 2 d^{-1} on the basis of the presence of snowfall in the watershed as predicted by SMDR. The wash-off coefficient ($k_{I,R}$) (equation (8)) was set a priori to

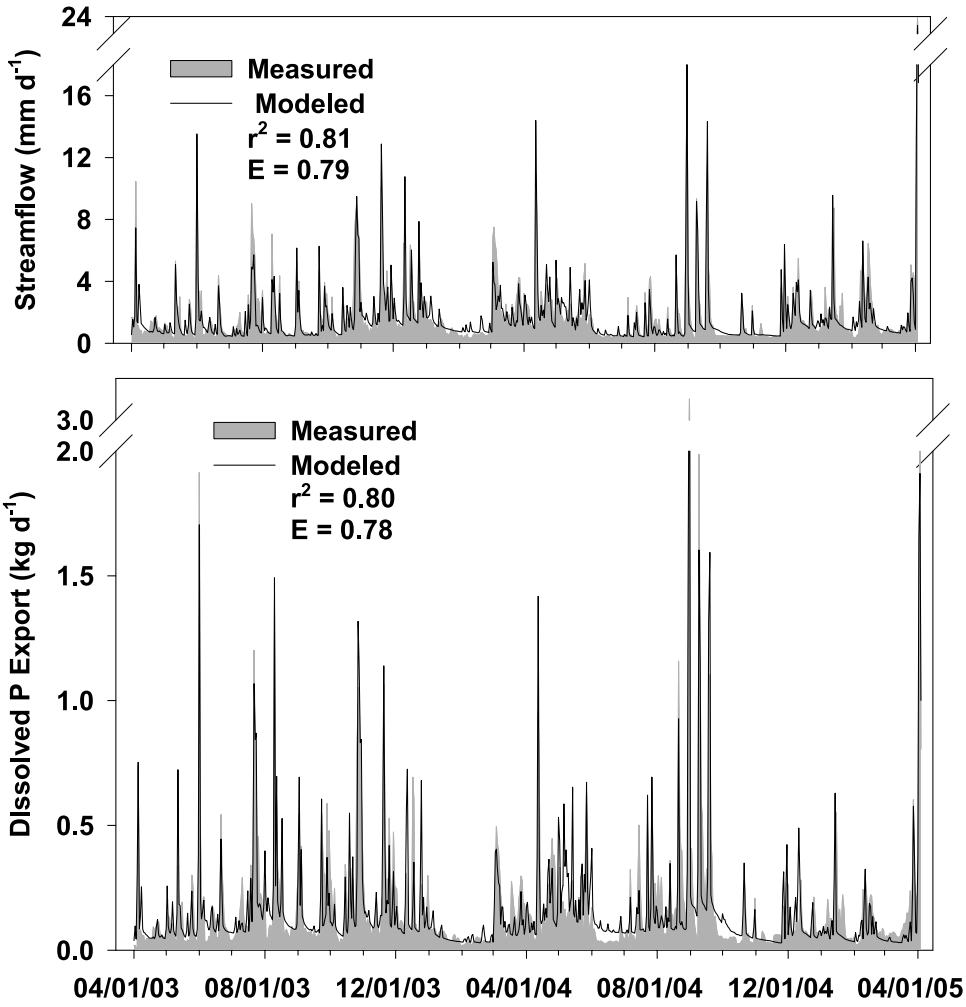

Figure 3. (top) Measured and modeled (SMDR predicted) streamflow at the watershed outlet. (bottom) Measured and modeled dissolved P (DP) loads at the watershed outlet. Total measured streamflow was 1247 mm, and total modeled streamflow (SMDR predicted) was 1232 mm.

0.02 m^2 m^{-3}, from measurements and values in the literature [*Sartor and Boyd*, 1972; *Alley*, 1981].

[28] The base temperature for soil (T_S) (equation (5)) was set a priori to the amplitude of monthly average temperature at the soil surface (20°C). The base temperature for base flow (T_B) (equation (10)) was set a priori to the amplitude of monthly average temperature at a depth of 50 cm (17°C) or, approximately the mean soil depth for the basin. The Q_S parameter (equation (5)) for soil was set by calibration with observed DP loads. The base flow export coefficient ($\mu_{T,B}$) (equation (10)) was taken from measured base flow DP loss, and the Q_B parameter (equation (9)) for base flow was set by calibration with low-flow events during 2003–2004. Table 2 lists calibrated parameters, and those taken directly from data sources.

7. Results

7.1. Validation

[29] Streamflow and landscape runoff losses were modeled in SMDR [*Easton et al.*, 2007] and used as drivers for the DP loading model. Two years of observed stream DP measurements were compared to modeled stream DP losses using visual methods (DP hydrograph) and various statistical methods including the Nash Sutcliffe efficiency (E) [*Nash and Sutcliffe*, 1970], and the coefficient of determination (r^2). Modeled and observed DP losses from the landscape were compared to assess the ability of the model to predict the distributed extent of DP source areas as well as the contributions of various landscapes in the watershed. The appropriate equation from the model development section was used to predict the DP loss from the landscapes. If the location of the plot in the landscape is on a fertilized area then contributions from fertilizer and the plant-soil complex are considered (i.e., equations (3) and (6) are used), if it is in an unfertilized area then only the plant-soil complex equations are used (equation (6). Distributed DP losses were compared for four runoff events over 13 d, spanning a wide range of precipitation depths and types (i.e., low-intensity precipitation, snowmelt, and intense thunderstorms).

7.2. Stream Phosphorus Load

[30] Figure 3 shows the daily measured and modeled streamflow and DP loads at the watershed outlet for April 2003 to April 2005. Data from 2003–2004 were used for calibration and data from 2004–2005 for validation. The

Table 3. Measured and Modeled Mean Daily Dissolved Phosphorus Loads in the Stream at the Watershed Outlet

Period[a]	Measured, kg d^{-1}	Modeled, kg d^{-1}	r^{2b}	E[c]
Summer 2003	0.186	0.181	0.82	0.81
Winter 2003–2004	0.138	0.134	0.59	0.50
Summer 2004	0.211	0.208	0.82	0.82
Winter 2004–2005	0.118	0.113	0.84	0.81
Summer mean	0.198	0.194	0.82	0.82
Winter mean	0.128	0.124	0.73	0.68
Overall mean	0.166	0.162	0.80	0.78

[a]Summer is May–October; winter is November–April.
[b]Coefficient of determination.
[c]Nash-Sutcliffe efficiency.

results of the statistical comparison (Table 3) indicate that the model predicts DP loads well on an overall basis (r^2 = 0.80, E = 0.78). In most cases, when the modeled and measured streamflow matched, the DP loads in the stream were accurately predicted (Figure 3 and Table 3). Some of the error can be attributed to errant snowmelt runoff predictions, a chronic weakness of SMDR. However, there may be processes that we failed to consider in the model that introduce error during these snowmelt events. Additionally, SMDR does not model infiltration excess runoff on soils (only saturation excess), so intense thunderstorms on dry summer soils can cause some error. For instance a thunderstorm on 16 July 2004 caused 8 mm of runoff, while SMDR predicted 6 mm and subsequently under predicted the DP load in the stream by 22% (Figure 3). During events dominated by saturation excess runoff the model preformed well, load peaks were correctly timed, and within 10% of the observed DP load. Both storm and base flow DP loads were modeled well, indicating that the model is capable across a wide range of conditions with little calibration (Figure 3).

[31] The statistics for the calibration year (2003–2004) show somewhat lower predictive capacity than for the validation year (2004–2005) (Table 3). Much of the disparity in the first year of simulation was due to several intense convective type thunderstorms which may have exceeded the infiltrative capacity of the dry soil in the summer. Winter 2003–2004 was characterized by several strictly snowmelt runoff events and several rainfall/snowmelt events (Figure 3). Because of the simple snowmelt algorithm in SMDR, together with large elevation differences and south facing slopes, snowmelt runoff has commonly been difficult to predict, particularly when temperatures fluctuate around freezing [*Frankenberger et al.*, 1999; *Mehta et al.*, 2004]. Furthermore, during the winter, temperature and snowfall data were collected off site, which can introduce error into the simulation [*Hively et al.*, 2005; *Gérard-Marchant et al.*, 2005a].

[32] In the second year of simulation (2004–2005) modeled DP loads better matched observed loads, as indicated by a visual inspection of Figure 3 and the statistics in Table 3. For summer 2004 both the r^2 and the E were 0.82, while for winter 2004 – 2005, they were 0.84 and 0.81 respectively, substantial improvements over the previous year. The five largest DP loads were all measured in the second year of the study. Except for one event on 18 September 2004 the modeled DP loads were within 10% of the observed DP loads (Figure 3). The 18 September 2004 event (under predicted by 21%) was mainly a result of a 20% under predicted streamflow by SMDR.

7.3. Distributed Dissolved P Loss From the Landscape

[33] The model captured the DP loss from the landscape well in the watershed with an E of 0.82 and r^2 of 0.83 (Table 4 and Figure 4). While there is some variability in the fit of the modeled data around the 1:1 line in Figure 4, there is no systematic deviation, indicating the little bias. Below we present and discuss four distinct noncalibration storm events to assess model predictions.

[34] Figure 5a shows DP losses on four sampling dates over a 1-week period (18–24 July 2003) during which 148 mm of precipitation fell. In general, if the runoff losses were well predicted, the DP losses tended to be captured accurately as well. Dissolved P loss from 18–20 July on landscapes 2, 6, and 9 were under predicted. Landscape 2 was under predicted because SMDR predicted 36% less

Table 4. Summary Statistics for Measured and Modeled Dissolved P Loss From Four Runoff Events Over 13 d Taken From the Landscape Sampling Locations[a]

	Measured, kg ha^{-1}			Modeled, kg ha^{-1}				
Event	Minimum	Mean[b]	Maximum	Minimum	Mean	Maximum	r^{2c}	E[d]
July 2003[e]	<0.01	0.07	0.16	0.00	0.06	0.18	0.78	0.71
Aug 2004[f]	0.01	0.07	0.14	<0.01	0.05	0.12	0.82	0.64
Sept 2004[g]	<0.01	0.02	0.03	<0.01	0.02	0.05	0.89	0.80
Mar–Apr 2005[h]	0.01	0.05	0.12	0.01	0.05	0.12	0.83	0.85
Overall	<0.01	0.07	0.16	0.00	0.06	0.18	0.83	0.82

[a]For sampling locations, see Figure 2.
[b]Values are calculated on an event basis, not by individual day.
[c]Coefficient of determination.
[d]Nash-Sutcliffe efficiency.
[e]Event consisted of four sampling dates.
[f]Event consisted of three sampling dates.
[g]Event consisted of two sampling dates.
[h]Event consisted of four sampling dates.

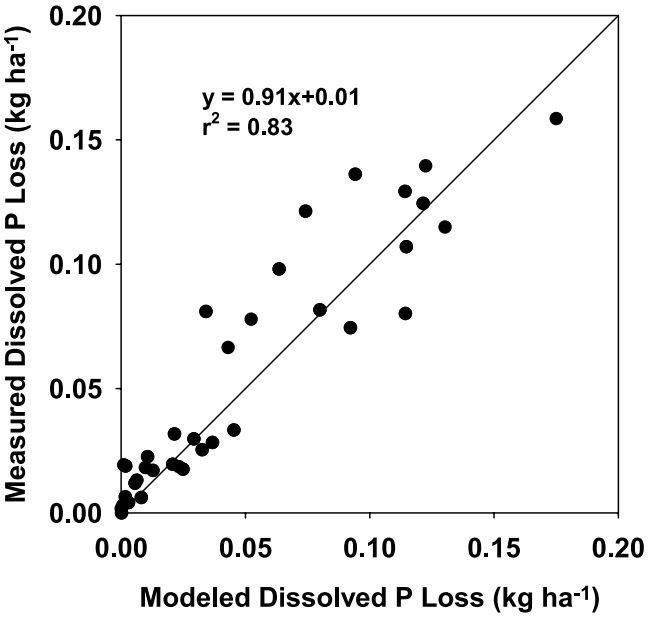

Figure 4. Measured and modeled landscape dissolved P (DP) loss from four runoff events in July 2003, August 2004, September 2004, and March–April 2005.

runoff form the landscape than was measured, a result of an intense thunderstorm. Indeed, substituting the observed for the predicted runoff resulted in much better predictions for these events (data not shown). While runoff was correctly predicted for landscapes 6 and 9 (both fertilized), the under estimation of DP loss may be due to the immobilization rate (τ) in equation (1) being set too high (9 d) or the available water extractable P (M_F) per application being too low (5.4×10^{-4} kg m^{-2}) (equation (2)). The following days (22–24 July) rainfall intensities were low and runoff was generated predominately by saturation excess processes, which SMDR predicted well and the DP loss was also well predicted (Figure 5a).

[35] The 29–31 August 2004 event was generally well predicted by the model across all three sampling dates (E = 0.64, r^2 = 0.82) (Figure 5b and Table 4), particularly the fertilized landscapes (landscapes 3 and 6). Fertilization was simulated two weeks prior to this event, so concentrations were high, but runoff losses were relatively low (2–6 mm $event^{-1}$ on fertilized landscapes), resulting in DP losses on the same order of magnitude as the losses from soils (where runoff losses averaged 10.8 mm $event^{-1}$). The errors on landscapes 2, 4, and 5 are mainly due to miss-predicted runoff. Again, substituting observed for predicted runoff corroborated this.

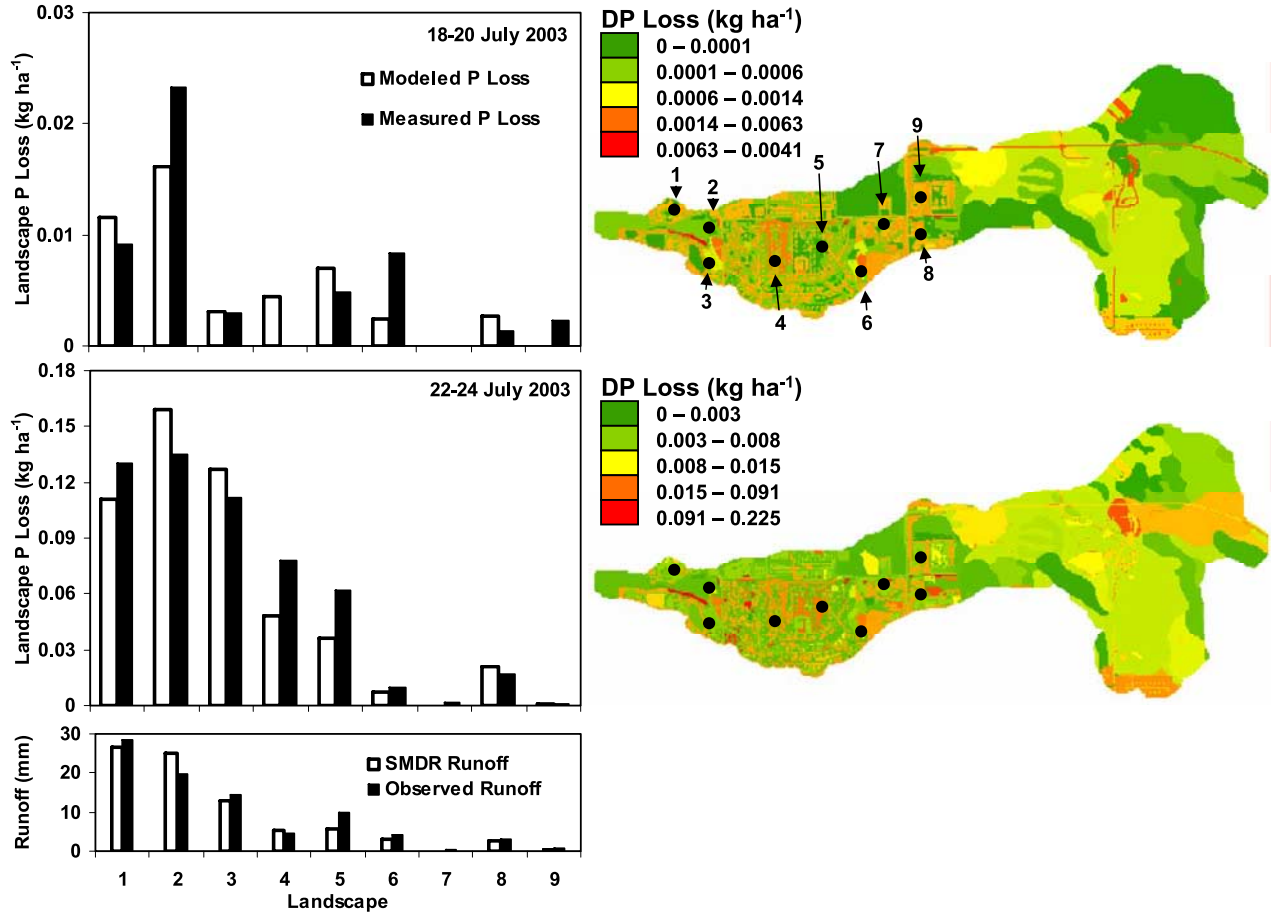

Figure 5a. (top and middle) Measured and modeled landscape dissolved P (DP) losses from the landscape sampling locations in Figure 2 for runoff events in July 2003. (bottom) SMDR predicted runoff used in the model. Maps at right show the predicted spatial distribution of DP loss corresponding to the adjacent plots. See Table 4 for statistical comparison of measured and modeled DP loss.

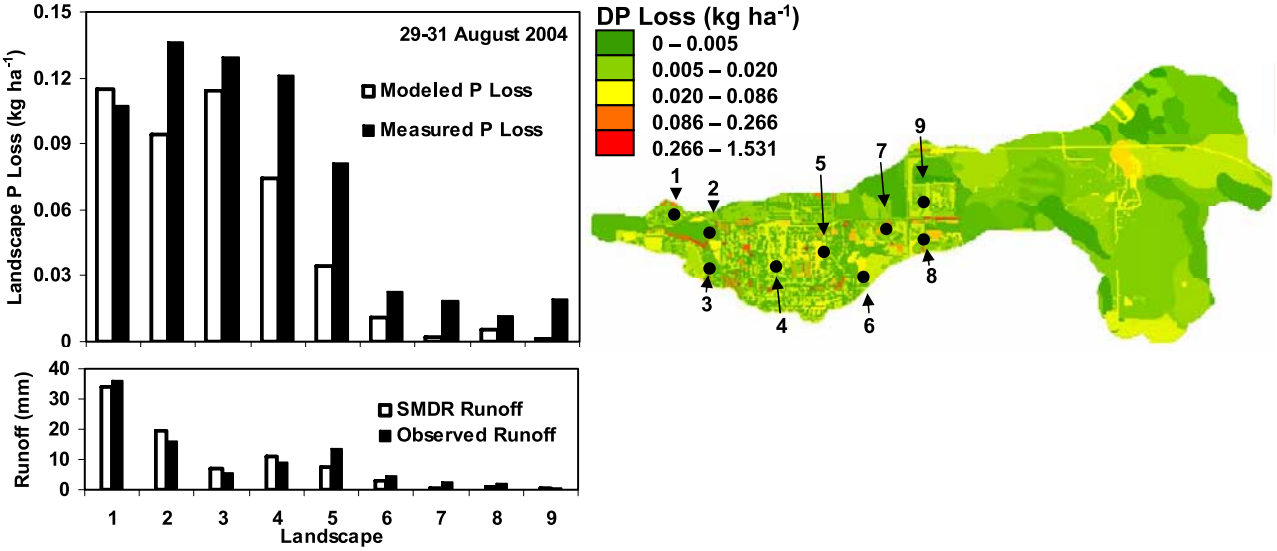

Figure 5b. (top) Measured and modeled landscape dissolved P (DP) losses from the landscape sampling locations in Figure 2 for runoff event in August 2004. (bottom) SMDR predicted runoff used in the model. Map at right shows the predicted spatial distribution of DP loss corresponding to the adjacent plot. See Table 4 for statistical comparison of measured and modeled DP loss.

[36] Similar to the August event, the 18–19 September 2004 event was well modeled with an E of 0.80 and an r^2 of 0.89 (Figure 5c and Table 4), particularly the fertilized landscapes (3, 6, and 9). Soils were at or close to saturation because of 30 d antecedent precipitation of 215 mm. Thus the 56 mm of precipitation on 18–19 September caused significant saturation excess runoff, and high DP losses particularly from the more heavily developed area of the watershed where soils are shallow (Table 1) and impervious surfaces abundant (Figure 2).

[37] The final event during the course of the study is shown in Figure 5d. This event in March and April 2005 consisted of snowmelt (29 March to 1 April) in addition to 111 mm of precipitation (2–4 April), which the statistical measures indicate was captured well on an overall basis (E = 0.85, r^2 = 0.83) (Table 4). The 29 March to 1 April 2005 portion of the event consisted almost entirely of snowmelt runoff, which contained significant P loads (Figure 5d). This is not unexpected, since freeze-thaw cycles occur often in this region, and can stimulate the release and availability of P [*Bechmann et al.*, 2005; *Freppaz et al.*, 2007].On 2–4 April 2005 the majority of the runoff was due to low-intensity precipitation and thus DP loss was predicted moderately well in the lower and

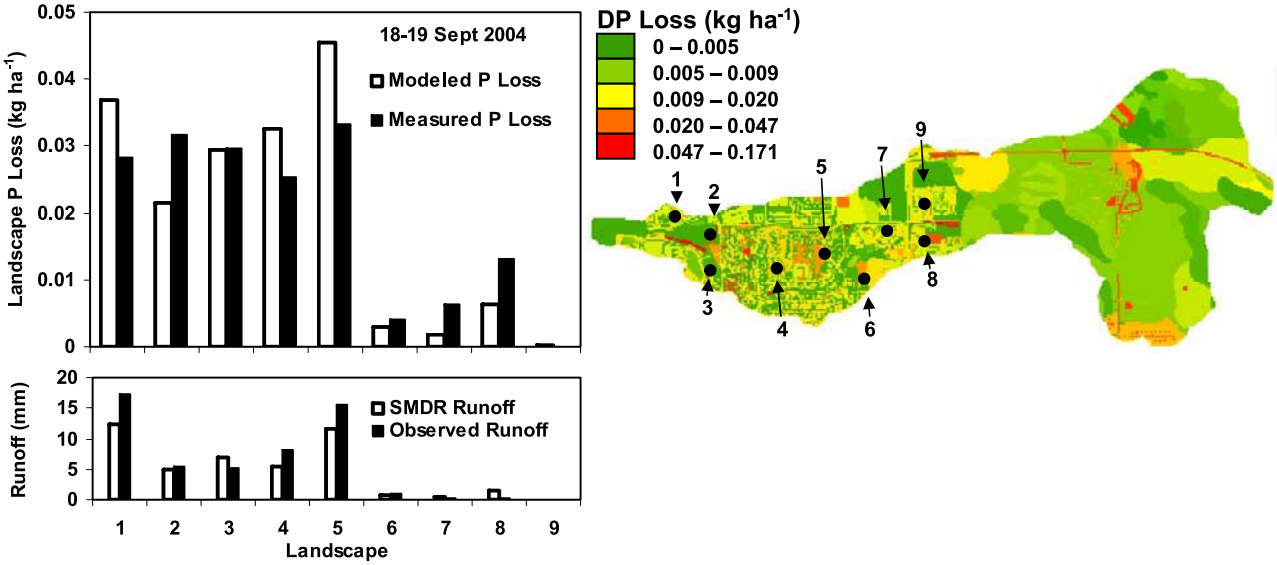

Figure 5c. (top) Measured and modeled landscape dissolved P (DP) losses from the landscape sampling locations in Figure 2 for runoff event in September 2004. (bottom) SMDR predicted runoff used in the model. Map at right shows the predicted spatial distribution of DP loss corresponding to the adjacent plot. See Table 4 for statistical comparison of measured and modeled DP loss.

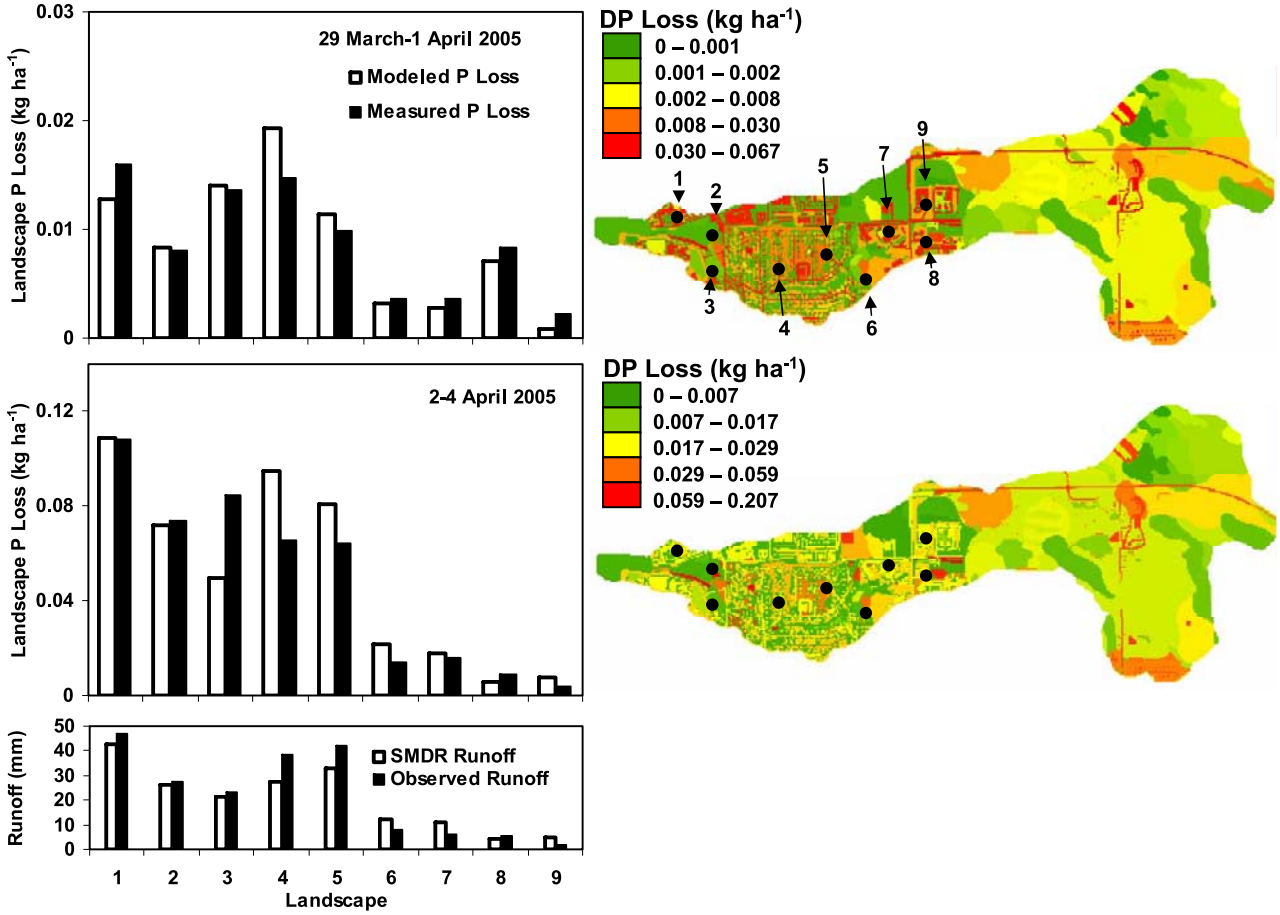

Figure 5d. (top and middle) Measured and modeled landscape dissolved P (DP) losses from the landscape sampling locations in Figure 1 for runoff event in March–April 2005. (bottom) SMDR predicted runoff used in the model. Map at right shows the predicted spatial distribution of DP loss corresponding to the adjacent plots. See Table 4 for statistical comparison of measured and modeled DP loss.

upper watershed (landscapes 1, 2, 6, 7, 8 and 9), but overestimated on the middle watershed (landscapes 3, 4, and 5) (Figure 5d).

[38] For all events, the highest DP loads are modeled as occurring in the middle and lower areas of the watershed (landscapes 1–5), consistent with measured DP losses.

8. Discussion

8.1. Landscape Processes

[39] The average concentration of DP at the outlet of this urban watershed is in excess of the 20 μg L^{-1}, which is thought to cause algal blooms in New York State [*Owens et al.*, 1998]. Therefore it is of interest to identify P source areas or particular management practices that contribute to high P loss. Approximately 2/3 of the modeled DP load (65%) is from surface runoff and the remainder is contributed by base flow (Table 5). The fertilized areas had the largest relative contribution in surface runoff (29% of the total in surface runoff or 19% of the total load in the stream) but cover only 8% of the watershed. Technically the P loss from fertilized areas can be separated into two components, P contributed directly by the fertilizer, and indirectly by the higher P concentration in the soil due to past fertilizer applications [*Sharpley and Syers*, 1983; *Sharpley et al.*, 2001; *McDowell et al.*, 2001; *Andraski and Bundy*, 2003]. The effect of this increase in STP levels is captured by the export coefficient, μ_S, from the plant-soil complex, and can be seen in Figure 2, where fertilized landscapes had the highest export coefficients as well as measured STP levels.

Table 5. Relative Contributions From Each Modeled Component to the Total Dissolved P Load in the Stream[a]

Period[b]	Impervious	Fertilized	Fertilized Soil[c]	Soil	Base Flow
Summer 2003	2.96	4.19	4.31	12.21	15.17
Winter 2003–2004	3.44	0.22	3.25	10.98	7.65
Summer 2004	2.23	3.55	4.25	12.79	14.40
Winter 2004–2005	3.07	0.01	2.44	8.07	5.38
Summer	5.19	7.74	4.28	29.28	29.57
Winter	6.51	0.23	2.85	21.90	13.03
Overall	11.70	7.97	14.26	44.05	42.60
Percent of total DP loss	10	7	12	36	35
Percent of watershed	10	8	8	82	-

[a]Relative contributions are given in kg.
[b]Summer is May–October-; winter is November–April.
[c]Value represents the contribution from soil under fertilized landscapes.

Both modeled and observed P loss from fertilizer were relatively high following fertilizer application. In some cases the model predicted fertilizer contributions to be as much as 75% of the total daily DP export, but availability and thus loss declined rapidly because of conversion to less soluble forms.

[40] The next largest contributor to the DP load in the stream were the impervious surfaces that covered 10% of the watershed area and contributed 10% of the total load (or 15% of the load in the runoff). For a sewered watershed in which the storm sewers outlet to a nearby stream or water body the contribution from impervious surfaces would have been much higher because approximately 37% of the runoff from the impervious surfaces reinfiltrated in surrounding landscape. Therefore, in Table 5, the total contribution from impervious surfaces is likely underestimated, but would be incorporated in to the losses estimated from the plant-soil complex. The rest of the landscape 82% (plant-soil complex), is unfertilized and pervious and contributes comparatively little to the total DP loss (36%). Somewhat misleading in Table 5 is that the DP loss from the soil was higher in the summer than in the winter (29 versus 22 kg). This is a direct consequence of the greater availability of P during the growing season from increased microbial activity and the wetter than normal summers which increased runoff compared to normal dryer years.

[41] DP contributions from base flow were 35% of the total DP load, but varied seasonally as well, higher in the summer and lower in the winter, reflecting both the elevated DP concentrations during the summer and the wetter than average years. During normal years there is little base flow in this watershed. The model is regrettably unable to capture the effect of urbanization on base flow concentration since the concentration is a lumped parameter which is calibrated from observed data. Compared with surrounding undeveloped watersheds the concentrations in the base flow are relatively high, indicating that urban areas have a greater effect on subsurface parameters than previously thought.

8.2. Effects of Urbanization

[42] In urbanizing watersheds the fraction of impervious area increases greatly, therefore it is important to study their impact in greater detail. During most events the influence of impervious surface DP wash-off, and the subsequently higher DP losses from surrounding landscapes is most apparent during the initial portion of the storm (18–20 July in Figure 5a and 29 March to 1 April in Figure 5d) where the DP that had accumulated on the impervious surfaces was flushed to the surrounding landscape and both the model and the measured data shows high DP losses. The DP contribution from impervious surfaces for storm events lasting more than several days (i.e., July 2003 and March–April 2005) declined substantially as the event progresses (Figures 5a and 5d), a result of continued IER preventing P accumulation. However, these long-duration events dramatically increased DP losses from the surrounding landscapes where significant levels of saturation excess runoff were generated and thus high quantities of DP were mobilized. Additionally, the IER from the impervious surfaces prolong the duration of saturated soils which tends to create a reducing environment and thus further increases DP loss [*Young and Ross*, 2001].

[43] Some of the underpredictions in the winter (Figure 3) may be a result of the buildup rate (k_1) on impervious surfaces being set too high for snowfall events in equation (7). This retards P accumulation on the impervious surface and lowers DP loss. Decreasing the buildup factor, k_1, improved predictions for some larger winter events, but resulted in over predictions smaller snowfall events. This indicates that application of deicing and traction material to roadways in the winter is proportional to snowfall event size/duration. Additionally, the deposition of P to impervious surfaces was assumed equal regardless of the impervious surface (i.e., roads, roofs, parking lots), which may not adequately capture the true dynamics of the DP load available on any one cell. For instance, state route 13 traverses a portion of the watershed and is most likely more heavily treated with deicing materials than other, smaller roads. Indeed, *Waschbusch et al.* [1999] reported that feeder streets produced more DP than collector or arterial streets in portions of Madison, WI. Additionally, DP deposition on roofs should be lower than on roadways. In fact, several grab samples of IER from roadways measured >2.5 mg P L^{-1}, while samples from driveways and roofs were in the 0.5–1 mg P L^{-1} range. However, because of limitations of model resolution distinguishing among impervious surfaces was unrealistic for this application, but could be implemented if data were available.

8.3. Effectiveness of Management Practices

8.3.1. Pervious Areas

[44] In order to reduce the contribution of P to the stream from the various landscapes in this and many other urban watersheds the spatial distribution of DP source areas in the landscape is an important consideration. In this watershed, fertilization as a whole, does not necessarily contribute to high losses, but rather fertilization in specific areas of the watershed can be problematic. For instance, in this watershed, landscapes 6, 7, 8, and 9 all had relatively high STP levels (Figure 2) (6 and 9 were fertilized), but had low runoff losses, and subsequently low DP losses (Figures 5a, 5b, 5c, and 5d), a result of deep, conductive soils (Table 1) and a small upslope contributing area. Conversely, landscapes 1, 2, 4 and 5 all had relatively low STP and were unfertilized, but consistently had the highest DP losses (Figures 5a, 5b, 5c, and 5d). Landscape 3 generally had lower runoff losses than landscapes 1, 2, 4, and 5 (Figures 5a, 5b, 5c, and 5d), but was fertilized, and thus had high DP losses. This indicates that both runoff production and P source areas are important to correctly predict to accurately capture the spatial extent and the timing of landscape DP loss. Thus a management practice (or a zoning ordinance) to prevent overfertilization of lawns in the high-runoff areas located near the existing streams would greatly reduce the loss of DP to the stream. Adjusting fertilizer timing to avoid wet periods would reduce DP losses as well. This is well illustrated, for example, by the sensitivity of the model to the fertilizer application rates in the late fall of both 2003 and 2004 (Figure 3) where the DP load in the stream was over predicted, perhaps because of the timing of the simulated fertilizer application in October. If this application is moved to September, or not simulated at all, the results improve substantially for the late fall but the DP loads for the early winter are low (not shown). Other

best management practices to reduce DP loss include reducing P fertilization of lawns, moving the typical late fall P application to an earlier date, avoiding fertilizer application prior to or during wet periods, and reducing P application to high STP soils.

8.3.2. Impervious Areas

[45] For impervious areas the results from this model indicate that management efforts to reduce nonpoint source DP loading to surface waters should focus on reducing DP loss during the winter when there is a large contribution of P from road salt/sand mixtures that have relatively high DP levels. Municipalities should consider using sand/salt mixtures with a low P content, alternative deicing products such as those using Cl^- (although there are tradeoffs with increasing Cl^- levels) [*Albright*, 2005] or implementing street sweeping on a more frequent basis. Frequent cleaning of street debris could reduce the DP load available for transport in runoff and reduce the total DP load in the stream considerably. This was not considered here because there is very limited street sweeping in this watershed, but could easily be added to the model if data were available.

9. Conclusions

[46] A distributed model was used to predict DP loss in an urban watershed. Runoff from the landscape and base flow were predicted by SMDR with 10 m resolution. Dissolved P losses in overland flow from soil and base flow were estimated with an export coefficient model adjusted for temperature using an Arrhenius equation. Export coefficients for plant-soil complexes were estimated from STP and DP runoff from soils in the watershed. Base flow losses were calibrated from measured base flow concentrations in the stream. Dissolved P loss in runoff from fertilized areas was simulated using the water soluble P in the fertilizer. Dissolved P loss from impervious surfaces was simulated using a deposition wash-off equation with consideration for seasonal P dynamics.

[47] When streamflow was correctly modeled the in-stream DP loads tended to be quite accurate. The largest contributor to DP loading in the stream was DP loss in overland flow from the plant-soil complex, followed by base flow, impervious surfaces, and fertilized areas. However, the dynamics of DP loss from all components varied spatially as well as temporally. Dissolved P loss from the plant-soil complex was highest during prolonged durations of saturated soil where runoff was abundant and where past fertilization had increased P levels. Fertilized areas contributed the highest DP loads directly following simulated application, while DP loss from the impervious surfaces were highest in the winter when significant quantities of P can accumulate from application of deicing materials. Base flow DP contributions were higher in the summer than winter reflecting the affect of temperature on P availability and the higher than average rainfall during the study period.

[48] The largest DP source areas in this watershed occur in the more heavily urbanized area near the outlet where impervious surfaces are abundant; soils are shallow and runoff losses high. This model was able to identify these critical source areas in the landscape with good accuracy and corroborate recent claims that effective watershed management should focus on the coincidence of pollutant source and runoff generating areas. This model provides information that can help watershed managers target storm water management strategies at parts of the landscape particularly prone to generating high DP losses, including assessing the suitability of certain activities in high-runoff generating areas of the watershed.

References

Ahmed, A. E., J. G. Arnold, J. Feyen, and J. Berlamont (2005), Modeling the hydrology of a catchment using a distributed and a semi-distributed model, *Hydrol. Processes*, *19*, 573–587.

Ahn, H., and R. T. James (2001), Variability, uncertainty, and sensitivity of phosphorus deposition load estimates in south Florida, *Water Air Soil Pollut.*, *126*, 37–51.

Albright, M. (2005), Changes in water quality in an urban stream following the use of organically derived deicing products, *Lake Reservoir Manage.*, *21*, 119–124.

Alley, W. (1981), Estimation of impervious area washoff parameters, *Water Resour. Res.*, *17*, 1161–1166.

Andraski, T. W., and L. G. Bundy (2003), Relationships between phosphorus levels in soil and in runoff from corn production systems, *J. Environ. Qual.*, *32*, 310–316.

Arnold, J. G., and N. Fohrer (2005), SWAT2000: Current capabilities and research opportunities in applied watershed modeling, *Hydrol. Processes*, *19*, 563–572.

Banks, H. H., and J. E. Nighswander (1999), Relative contribution of hemlock pollen to the phosphorus loading of the Clear Lake ecosystem near Minden, Ontario, paper presented at Symposium on Sustainable Management of Hemlock Ecosystems in Eastern North America, For. Serv., U. S. Dep. of Agric., Durham, N. H.

Bannerman, R. T., D. W. Owens, R. B. Dodds, and N. J. Hornewer (1993), Sources of pollutants in Wisconsin stormwater, *Water Sci. Technol.*, *28*, 241–259.

Beauchemin, S., R. R. Simard, and D. Cluis (1996), Phosphorus sorption-desorption kinetics of soil under contrasting land uses, *J. Environ. Qual.*, *25*, 1317–1325.

Bechmann, M. E., P. J. A. Kleinman, A. N. Sharpley, and L. S. Saporito (2005), Freeze-thaw effects on phosphorus loss in runoff from manured and catch-cropped soils, *J. Environ. Qual.*, *34*, 2301–2309.

Beven, K. (1996), A discussion of distributed hydrologic modeling, in *Distributed Hydrologic Modeling*, edited by M. Abbott and J. C. Refsgaard, pp. 255–277, Kluwer, Dordrecht, Netherlands.

Borah, D. K., and M. Bera (2004), Watershed-scale hydrologic and nonpoint-source pollution models: Review of applications, *Trans. ASAE*, *47*, 789–803.

Burian, S. J., T. N. McPherson, M. J. Brown, G. E. Streit, and H. J. Turin (2002), Modeling the effects of air quality policy changes on water quality in urban areas, *Environ. Monit. Assess.*, *7*, 179–190.

Caruso, B. S. (2000), Spatial and temporal variability of stream phosphorus in a New Zealand high-country agricultural catchment, *N. Z. J. Agric. Res.*, *43*, 235–249.

Cassell, E. A., N. F. Dorioz, R. L. Kort, J. P. Hoffmann, D. W. Meals, D. Kirschtel, and D. C. Bruan (1989), Modeling phosphorus dynamics in ecosystems: Mass balance and dynamic simulation approaches, *J. Environ. Qual.*, *27*, 293–298.

DeLaune, P. B., P. A. Moore, D. K. Carman, A. N. Sharpley, B. E. Haggard, and T. C. Daniel (2004a), Development of a phosphorus index for pastures fertilized with poultry litter—Factors affecting phosphorus runoff, *J. Environ. Qual.*, *33*, 2183–2191.

DeLaune, P. B., P. A. Moore, D. K. Carman, A. N. Sharpley, B. E. Haggard, and T. C. Daniel (2004b), Evaluation of the phosphorus source component in the phosphorus index for pastures, *J. Environ. Qual.*, *33*, 2192–2200.

Djodijc, F., K. Borling, and L. F. Bergstrom (2004), Phosphorus leaching in relation to soil type and soil phosphorus content, *J. Environ. Qual.*, *33*, 678–684.

Dorney, J. R. (1985), Leachable and total phosphorus in urban street tree leaves, *Water Air Soil Pollut.*, *28*, 439–443.

Dougherty, M., R. L. Dymond, T. J. Grizzard, A. N. Godrej, C. E. Zipper, and J. Randolph (2006), Quantifying long-term NPS pollutant flux in an urbanizing watershed, *J. Environ. Eng. Am. Soc. Civ. Eng.*, *132*, 547–554.

Dougherty, M., R. L. Dymond, T. J. Grizzard, A. N. Godrej, C. E. Zipper, and J. Randolph (2007), Quantifying long-term hydrologic response in an urbanizing basin, *J. Hydrol. Eng.*, *12*, 33–41.

Easton, Z. M., and A. M. Petrovic (2004), Fertilizer source effect on ground and surface water quality in drainage from turfgrass, *J. Environ. Qual.*, *33*, 645–655.

Easton, Z. M., and A. M. Petrovic (2007), Determining nutrient loading rates based on land use in an urban watershed: Phosphorus, in *The Fate of Nutrients and Plant Protection Chemicals in the Urban Environment*, edited by A. M. Petrovic and B. P. Horgan, Am. Chem. Soc., Washington, D. C., in press.

Easton, Z. M., P. Gérard-Marchant, M. T. Walter, A. M. Petrovic, and T. S. Steenhuis (2007), Hydrologic assessment of an urban variable source watershed in the northeast United States, *Water Resour. Res.*, *43*, W03413, doi:10.1029/2006WR005076.

Edwards, D. R., and T. C. Daniel (1994), A comparison of runoff quality effects of organic and inorganic fertilizers applied to fescuegrass plots, *Water Resour. Bull.*, *30*, 35–41.

Ekholm, P., K. Kallio, S. Salo, O. P. Pietilainen, S. Rekolainen, Y. Laine, and M. Joukola (2000), Relationship between catchment characteristics and nutrient concentrations in an agricultural river system, *Water Res.*, *34*, 3709–3716.

Endreny, T. A., and E. F. Wood (1999), Distributed watershed modeling of design storms to identify nonpoint source loading areas, *J. Environ. Qual.*, *28*, 388–397.

Evans, D. J., and P. Johnes (2004), Physico-chemical controls on phosphorus cycling in two lowland streams. part 1—The water column, *Sci. Total Environ.*, *329*, 145–163.

Frankenberger, J. R., E. S. Brooks, M. T. Walter, M. F. Walter, and T. S. Steenhuis (1999), A GIS-based variable source area hydrology model, *Hydrol. Processes*, *13*, 805–822.

Freppaz, M., B. L. Williams, A. C. Edwards, R. Scalenghe, and E. Zanini (2007), Simulating soil freeze/thaw cycles typical of winter alpine conditions: Implications for N and P availability, *Appl. Soil Ecol.*, *35*, 247–255.

Frossard, E., L. M. Condron, O. A. S. Sinaj, and J. C. Fardeau (2000), Process governing phosphorus availability in temperate soils, *J. Environ. Qual.*, *29*, 15–23.

Gachter, R., J. M. Ngatiah, and C. Stamm (1998), Transport of phosphate from soil to surface waters by preferential flow, *Environ. Sci. Technol.*, *32*, 1865–1869.

Garn, H. S. (2002), Effects of lawn fertilizer on nutrient concentration in runoff from lakeshore lawns, Lauderdale Lakes, Wisconsin, *U.S. Geol. Surv. Water Res. Invest. Rep., 02-4130*, 6 pp.

Gérard-Marchant, P., W. D. Hively, and T. S. Steenhuis (2005a), Distributed hydrological modeling of total dissolved phosphorus transport in an agricultural landscape, part I: Distributed runoff generation, *Hydrol. Earth Syst. Sci. Discuss.*, *2*, 1537–1579.

Gérard-Marchant, P., M. T. Walter, and T. S. Steenhuis (2005b), Simple models for phosphorus loss from manure in runoff, *J. Environ. Qual.*, *34*, 872–876.

Gross, C. M., J. S. Angle, R. L. Hill, and M. S. Welterlen (1991), Runoff and sediment losses from tall fescue under simulated rainfall, *J. Environ. Qual.*, *20*, 604–607.

Hamilton, P. A., T. L. Miller, and D. N. Myers (2004), Water quality in the nation's streams and aquifers: Overview of selected findings, *U.S. Geol. Surv. Circ. 1265*, Washington, D. C., 19 pp.

Hansen, N. C., T. C. Daniel, A. N. Sharpley, and J. L. Lemunyon (2002), The fate and transport of phosphorus in agricultural systems, *J. Soil Water Conserv.*, *57*, 408–416.

Hernandez, M., S. N. Miller, D. C. Goodrich, B. F. Goff, W. G. Kepner, C. M. Edmonds, and K. B. Jones (2000), Modeling runoff response to land cover and rainfall spatial variability in semi-arid watersheds, *Environ. Monit. Assess.*, *64*, 285–298.

Hively, W. D., P. Gerard-Marchant, and T. S. Steenhuis (2005), Distributed hydrological modeling of total dissolved phosphorus transport in an agricultural landscape part II: Dissolved phosphorus transport, *Hydrol. Earth Syst. Sci. Discuss.*, *2*, 1581–1612.

Hooda, P. S., M. Moynagh, I. F. Svoboda, A. C. Edwards, H. A. Anderson, and G. Sym (1999), Phosphorus loss in drainflow from intensively managed grassland soils, *J. Environ. Qual.*, *28*, 1235–1242.

Hu, F. S., B. P. Finney, and L. B. Brubaker (2001), Effects of Holocene Alnus expansion on aquatic productivity, nitrogen cycling and soil development in southwestern Alaska, *Ecosystems*, *4*, 358–368.

Interlandi, S. J., and C. S. Crockett (2003), Recent water quality trends in the Schuylkill River, Pennsylvania, USA: A preliminary assessment of the relative influences of climate, river discharge and suburban development, *Water Res.*, *37*, 1737–1748.

Johnson, M. S., W. F. Coon, V. K. Mehta, T. S. Steenhuis, E. S. Brooks, and J. Boll (2003), Application of two hydrologic models with different runoff mechanisms to a hillslope dominated watershed in the northeastern US: A comparison of HSPF and SMR, *J. Hydrol.*, *284*, 57–76.

Kuo, W. L., T. S. Steenhuis, C. E. McCulloch, C. L. Mohler, and D. A. Weinstein (1999), Effect of grid size on runoff and soil moisture for a variable-source-area, *Water Resour. Res.*, *35*, 3419–3428.

Kussow, W. (2007), Nitrogen and soluble phosphorus losses from and Upper Midwest lawn, in *The Fate of Nutrients and Plant Protection Chemicals in the Urban Environment*, edited by A. M. Petrovic and B. P. Horgan, Am. Chem. Soc., Washington, D. C., in press.

Linde, D. T., and T. L. Watschke (1997), Nutrients and sediment in runoff from creeping bentgrass and perennial ryegrass turfs, *J. Environ. Qual.*, *87*, 176–182.

Maguire, R. O., and J. T. Sims (2002), Soil testing to predict phosphorus leaching, *J. Environ. Qual.*, *31*, 1601–1609.

Mamo, M., D. Ginting, C. W. Zanner, D. L. McCakister, R. R. Renken, and C. A. Shapiro (2005), Phosphorus stratification and potential for runoff toss following long term manure application, *J. Soil Water Conserv.*, *60*, 243–250.

McDowell, R. W., and A. N. Sharpley (2003), Phosphorus solubility and release kinetics as a function of soil test P concentrations, *Geoderma*, *112*, 143–154.

McDowell, R., A. Sharpley, and G. Folmar (2001), Phosphorus export from an agricultural watershed: Linking source and transport mechanisms, *J. Environ. Qual.*, *30*, 1587–1595.

McIntosh, J. J. (1969), Bray and Morgan soil extractants modified for testing acid soils from different parent materials, *Agron. J.*, *61*, 259–265.

Meals, D. W., and L. F. Budd (1998), Lake Champlain basin nonpoint source phosphorus assessment, *J. Am. Water Resour. Assoc.*, *34*, 251–265.

Mehta, V. K., M. T. Walter, E. S. Brooks, T. S. Steenhuis, M. F. Walter, M. Johnson, J. Boll, and D. Thongs (2004), Application of SMR to modeling watersheds in the Catskill Mountains, *Environ. Modeling Assess.*, *9*, 77–89.

Munroe, D. K., C. Croissant, and A. M. York (2005), Land use policy and landscape fragmentation in an urbanizing region: Assessing the impact of zoning, *Appl. Geogr.*, *25*, 121–141.

Murphy, J., and J. R. Riley (1962), A modified single solution method for the determination of phosphate in natural waters, *Anal. Chem.*, *27*, 37–46.

Nash, J. E., and J. V. Sutcliffe (1970), River flow forecasting through conceptual models. part I: A discussion of principles, *J. Hydrol.*, *10*, 282–290.

Nichols, D. J., T. C. Daniel, and D. R. Edwards (1994), Nutrient runoff from pasture after incorporation of poultry litter or inorganic fertilizer, *Soil Sci. Soc. Am. J.*, *58*, 1224–1228.

Norton, M. M., and T. R. Fisher (2000), The effects of forest on stream water quality in two coastal plain watersheds of the Chesapeake Bay, *Ecol. Eng.*, *14*, 337–362.

Owens, E. M., S. W. Effler, S. M. Doerr, R. K. Gelda, E. M. Schneiderman, D. G. Lounsbury, and C. L. Stepczuk (1998), A strategy for reservoir model forecasting based on historic meteorological conditions, *J. Lake Reservoir Manage.*, *14*, 322–333.

Puckett, L. J. (1995), Identifying the major sources of nutrient water-pollution, *Environ. Sci. Technol.*, *29*, A408–A414.

Rahman, M., and I. Salbe (1995), Modeling impacts of diffuse and point source nutrients on the water quality of South Creek catchment, *Environ. Int.*, *21*, 597–603.

Sartor, J., and G. Boyd (1972), Water pollution aspects of street surface contaminants, *Rep. EPA-R2-72-081*, U.S. Environ. Prot. Agency, Washington, D. C.

Shaheen, D. J. (1975), Contribution of urban roadway to water pollution, *Rep. EPA-6002-75-004*, Off. of Res. and Dev., U.S. Environ. Prot. Agency, Washington, D. C.

Sharpley, A. N. (1981), The contribution of phosphorus leached from crop canopy to losses in surface runoff, *J. Environ. Qual.*, *10*, 160–165.

Sharpley, A. N., and J. K. Syers (1983), Transport of phosphorus in surface runoff as influenced by liquid and solid fertilizer phosphate addition, *Water Air Soil Pollut.*, *19*, 321–326.

Sharpley, A. N., J. K. Syers, and P. E. H. Gregg (1978), Transport in surface runoff of phosphorus derived from dicalcium phosphate and superphosphate, *N. Z. J. Sci.*, *21*, 307–310.

Sharpley, A. N., R. W. McDowell, J. L. Weld, and P. J. A. Kleinman (2001), Assessing site vulnerability to phosphorus loss in an agricultural watershed, *J. Environ. Qual.*, *30*, 2026–2036.

Sharpley, A. N., P. J. Kleinman, G. M. R. McDowell, and R. B. Bryant (2002), Modeling phosphorus transport in agricultural watersheds: Process and possibilities, *J. Soil Water Conserv.*, *57*, 425–439.

Smart, M. M., T. W. Barney, and J. R. Jones (1981), Watershed impact on stream water quality: A technique for regional assessment, *J. Soil Water Conserv.*, *36*, 297–300.

Soranno, P. A., S. L. Hubler, S. R. Carpenter, and R. C. Lathrop (1996), Phosphorus loads to surface waters: A simple model to account for spatial pattern of land use, *Ecol. Appl.*, *6*, 865–878.

Srinivasan, M. S., P. Gerard-Marchant, T. L. Veith, W. J. Gburek, and T. S. Steenhuis (2005), Watershed scale modeling of critical source areas of runoff generation and phosphorus transport, *J. Am. Water Res. Assoc.*, *41*, 361–375.

Tarkelson, D. D., and R. L. Mikkelsen (2004), Runoff phosphorus losses as related to phosphorus source, application method and application rate on a Piedmont soil, *J. Environ. Qual.*, *33*, 1424–1430.

Tierney, J., and C. Silver (2002), Scientific guidance on lower phosphorus roadway deicers, general memorandum, Off. of N. Y. Attorney, 2 April. (Available at http://www.oag.state.ny.us/environment/deicer.html)

Tilley, D. R., and M. T. Brown (1998), Wetland networks for stormwater management in subtropical urban watersheds, *Ecol. Eng.*, *10*, 131–158.

Torrent, J., and A. Delgadao (2001), Using phosphorus concentrations in the soil solution to predict phosphorus desorption to water, *J. Environ. Qual.*, *30*, 1829–1835.

Tsihrintzis, V. A., and R. Hamid (1998), Runoff quality prediction from small urban catchments using SWMM, *Hydrol. Processes*, *12*, 311–329.

Tufford, D. L., C. L. Samarghitan, H. N. McKellar, D. E. Porter, and J. R. Hussey (2003), Impacts of urbanization on nutrient concentrations in small southeastern coastal streams, *J. Am. Water Res. Assoc.*, *39*, 301–312.

Tukey, H. B. J. (1970), The leaching of substance from plants, *Annu. Rev. Plant Physiol.*, *21*, 305–324.

Waschbusch, R. J., W. R. Selbig, and R. T. Bannerman (1999), Sources of phosphorus in stormwater and street dirt from two urban residential basins in Madison, Wisconsin, 1994–95, *U.S. Geol. Surv. Water Resour. Invest. Rep.*, *99-4021*.

Wayland, K. G., D. T. Long, D. W. Hyndman, B. C. Pijanowski, S. M. Woodhams, and S. K. Haack (2003), Identifying relationships between baseflow chemistry and landuse with synoptic sampling and R-mode factor analysis, *J. Environ. Qual.*, *32*, 180–190.

Winter, J. G., and H. C. Duthie (2000), Export coefficient modeling to assess phosphorus loading in an urban watershed, *J. Am. Water Res. Assoc.*, *36*, 1053–1061.

Young, E. O., and D. S. Ross (2001), Phosphate release from seasonally flooded soils: A laboratory microcosm study, *J. Environ. Qual.*, *30*, 91–228.

Zhang, H. P., and K. Yamada (1996), Estimation for urban runoff quality modeling, *Water Sci. Technol.*, *34*, 49–54.

Zheng, X. H., Y. Huang, Y. S. Wang, M. X. Wang, J. S. Jin, and L. T. Li (2003), Effects of soil temperature on nitric oxide emission from a typical Chinese rice-wheat rotation during the non-waterlogged period, *Global Change Biol.*, *9*, 601–611.

Z. M. Easton, T. S. Steenhuis, and M. T. Walter, Department of Biological and Environmental Engineering, Cornell University, Riley Robb Hall, Ithaca, NY 14853, USA. (zme2@cornell.edu)

P. Gérard-Marchant, Department of Biological and Agricultural Engineering, Driftmier Engineering Center, University of Georgia, Athens, GA 30602, USA.

A. M. Petrovic, Department of Horticulture, Plant Science Building, Cornell University, Ithaca, NY 14853, USA.